The solution structure of the SODD BAG domain reveals additional electrostatic interactions in the HSP70 complexes of SODD subfamily BAG domains

Christoph Brockmann[a,b], Dietmar Leitner[a], Dirk Labudde[a], Annette Diehl[a], Volker Sievert[c], Konrad Büssow[c], Ronald Kühne[a], Hartmut Oschkinat[a,b,*]

[a] *Forschungsinstitut für Molekulare Pharmakologie, Robert-Rössle-Str. 10, D-13125 Berlin, Germany*
[b] *Freie Universität, Berlin, Germany*
[c] *Max Planck Institut für molekulare Genetik, Berlin, Germany*

Received 12 November 2003; revised 8 December 2003; accepted 10 December 2003

First published online 15 January 2004

Edited by Thomas L. James

Abstract The solution structure of an N-terminally extended construct of the SODD BAG domain was determined by nuclear magnetic resonance spectroscopy. A homology model of the SODD-BAG/HSP70 complex reveals additional possible interactions that are specific for the SODD subfamily of BAG domains while the overall geometry of the complex remains the same. Relaxation rate measurements show that amino acids N358–S375 of SODD which were previously assigned to its BAG domain are not structured in our construct. The SODD BAG domain is thus indeed smaller than the homologous domain in Bag1 defining a new subfamily of BAG domains.

Key words: Silencer of death domains; Bcl-associated athanogene 4; Heat shock protein 70; Nuclear magnetic resonance structure; Homology model

1. Introduction

BAG (Bcl-associated athanogene) domains were recently identified as protein–protein interaction domains with low sequence similarity (Fig. 1) involved in apoptosis regulation [1]. They appear in a variety of vertebrate, insect, nematode, yeast and plant proteins [2]. Most of the known BAG domains were found to interact with the ATPase domain of heat shock protein (HSP) 70 and with the apoptosis regulator protein Bcl2 [2,3].

Silencer of death domains (SODD) is a BAG domain containing protein of 457 amino acids which was identified as a binding partner for the intracellular domains of tumor necrosis factor receptor 1 (TNF-R1) and death receptor 3 (DR3) [4]. SODD also interacts with Bcl2 via its BAG domain (residues 378–452) [3]. SODD was shown to act in an anti-apoptotic manner and was found to be overexpressed in pancreatic cancer cells [5]. It was recently hypothesized that the BAG domain also interacts with a predicted ATPase domain in TNF-R1 [6]. In contradiction, the N-terminal region of SODD interacted in the original two-hybrid screens with the death domains of TNF-R1 and DR3 [4]. Neither the mechanism of the antiapoptotic function of SODD nor the role of HSP70 in BAG domain-mediated apoptosis regulation and hence the role of the BAG/HSP70 interaction have been explained to date.

BAG domains form three-helix bundle structures [7–9]. The interaction interface of the hBag1 BAG domain in complex with HSP70 was analyzed by X-ray crystallography and is located at the interface of the second and third helices [8]. Nuclear magnetic resonance (NMR) studies on the mBag1 BAG domain with peptides derived from HSP70 were consistent with these results [7]. The interaction of BAG domains with Bcl2 was not investigated in detail so far. Only a BH3 binding motif homologous to a motif in the Bcl2 interacting protein Bax was hypothesized in BAG domains [3]. Recent structural studies [9] showed the SODD BAG domain to be smaller than its homologous domain in Bag1, defining a new subfamily of short SODD-like BAG domains. However, it was unclear whether the domains of this subfamily are really shorter or whether their N-terminal domain boundaries are only shifted towards the N-terminus.

In this work we report the NMR structure of an N-terminally extended SODD BAG domain construct accompanied by relaxation rate measurements to clarify domain boundaries. A homology model of the SODD-BAG/HSP70 complex was constructed to analyze SODD subfamily-specific contacts in the binding interface and to investigate differences in HSP70 binding of the two BAG domain subfamilies.

2. Materials and methods

2.1. Expression/purification

A DNA sequence encoding human SODD positions N358–G456 was cloned into a pGEX-P6 expression vector (Amersham Pharmacia). $^{13}C/^{15}N$-labeled protein was expressed in *Escherichia coli* in M9 minimal medium with ^{15}N-NH_4Cl or ^{15}N-NH_4Cl and u^{13}C-glucose (Campro) as only sources of nitrogen and carbon, respectively. Glutathione *S*-transferase affinity chromatography was applied for protein purification. The fusion protein was then cleaved by 1.25 U PreScission protease (Amersham Pharmacia) per mg protein overnight at 4°C, yielding the fragment GPLGS-N358-G456. Uncleaved protein was removed by gel filtration chromatography on a Superdex 75 column (Amersham Pharmacia). The fusion protein was concentrated to 15 mg/ml (1.3 mM) for NMR analysis.

*Corresponding author. Fax: (49)-30-94793 169.
E-mail address: oschkinat@fmp-berlin.de (H. Oschkinat).

Abbreviations: SODD, silencer of death domains; Bag, Bcl-associated athanogene; HSP, heat shock protein; NMR, nuclear magnetic resonance; NOE, nuclear Overhauser effect

0014-5793/04/$30.00
doi:10.1016/S0014-5793(03)01490-X

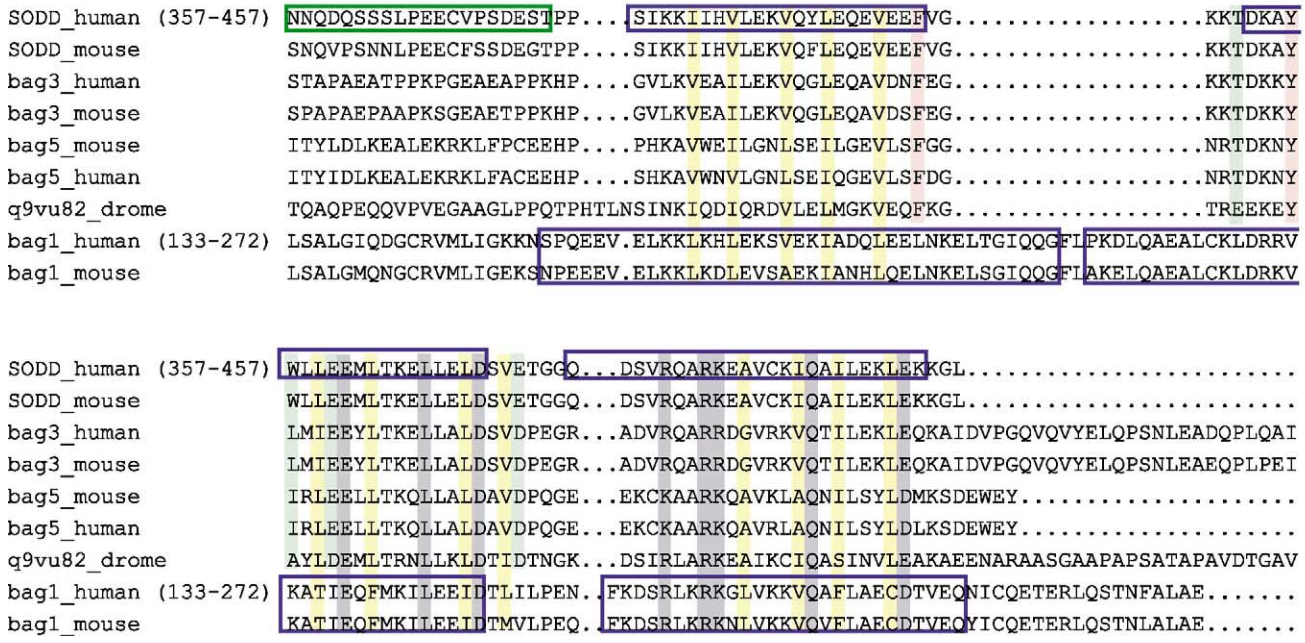

Fig. 1. Sequence alignment of selected BAG domains showing the difference between the SODD and the Bag1 subfamilies. SODD subfamily proteins are characterized by a 19 amino acid gap and the conserved residues homologous to F400 and Y409 in SODD, underlined in red. SODD subfamily-specific residues in the binding interface of the SODD subfamily are highlighted in green. The HSP70 binding residues present in all BAG domains are marked with gray boxes. Common hydrophobic core residues are in yellow. The α-helix positions in the structures of SODD, hBag1 and mBag1 BAG domains are given with the blue boxes. The green box shows the N-terminal unstructured region present in our construct. Note that the alignment includes only a subset of known BAG domains. Sequences were taken from the SwissProt database. Accession numbers from top: O95429, Q9CWG2, O95817, Q9JLV1, Q9DAU0, Q9UL15, Q9VU82, Q99933, Q60739.

2.2. NMR spectroscopy/structure calculation

NMR spectra were acquired at 27°C on a Bruker DRX600 spectrometer using a uniformly ^{15}N- and^{13}C-labeled sample containing 1.3 mM protein, 20 mM KH_2PO_4, 50 mM NaCl and 0.02% NaN_3 at pH 6.0 in 90% H_2O/10% D_2O. Spectra were processed using the XWINNMR software (Bruker Biospin). For backbone resonance assignments a complete series of side chain-selective ^{15}N-HSQC experiments [10–12] and triple resonance CBCA(CO)NH/CBCANH, HA(CACO)NH/HA(CA)NH and HNCO/HN(CA)CO spectra were used [13,14]. Side chain resonances were identified by combined evaluation of HBHA(CO)NH, H(CCCO)NH-TOCSY, (H)CC(CO)NH-TOCSY [15] experiments in H_2O and HCCH-TOCSY (for the aromatic-region) and HCCH-COSY [16] experiments in 100% D_2O. Side chains of Q and N were assigned using a series of side chain-NH_2-selective COSY spectra [17]. Inter-proton distance information for structure calculation was derived from ^{15}N-NOESY-HSQC [18], a methyl group-filtered ^{13}C-NOESY-HQQC, a 2D-^{1}H-^{1}H-NOESY [19] and a ^{13}C-NOESY-HMQC [18] spectrum. All NOESY spectra were acquired using 80 ms mixing time. The SPARKY software [20] was used for assignment of the spectra.

Relaxation rate measurements were performed as described previously [21]. Both T_1 and T_2 relaxation times were extracted from two series comprising each of 11 ^{1}H-^{15}N-HSQC type spectra with delays of 12, 52, 102, 152, 202, 302, 402, 602, 902, 2002, and 5002 ms for T_1 and 6, 10, 18, 26, 34, 42, 82, 122, 162, 202, and 242 ms for T_2. Rates and errors were fitted as implemented in the SPARKY software.

Secondary structure predictions were made using the chemical shift-based approaches of PLATON [22] and TALOS [23]. Chemical shift distributions of C^α and C^β chemical shifts were additionally analyzed according to the following equation [24]:

$$\Delta\Delta\delta_i = \frac{1}{3}\sum_{i-1}^{i+1}(\Delta\delta_{C\alpha_n} - \Delta\delta_{C\beta_n}) \quad (1)$$

where $\Delta\delta_{C\alpha_i}$ and $\Delta\delta_{C\beta_i}$ are the differences of the observed chemical shifts for C^α and C^β of an individual amino acid in SODD BAG and the random coil chemical shifts as obtained from BMRB.

Structures were calculated by the program CNS 1.01 [25]. A total of 731 nuclear Overhauser effect (NOE)-derived inter-residue distance restraints, 52 distance restraints mimicking H-bonds based on characteristic short-range NOE patterns, and 70 pairs of ϕ,ψ angle restraints generated by TALOS were used (see Table 1). Distance restraints were categorized in four classes: I: >3.5 Å, II: >4.7 Å, III: >5.5 Å and IV: >6.5. For analysis of the final ensemble MOLMOL [26] and Procheck-NMR [27] were used.

2.3. Computer modelling of the SODD-BAG/HSP70 complex

The SODD BAG domain was fitted into the hBag1 complex structure 1HX1 using the coordinates of the backbone atoms of amino acids 414, 420, 424, 438, 446 and 453. Side chain conformations of these residues were manually optimized to achieve the same contacts of the corresponding residues in the hBag1/HSP70 complex. Missing atoms in the crystal structure were added and this starting structure was minimized with AMBER5 [28] prior to the low restrained molecular dynamics simulation. For the minimization of the complex model all atoms of HSP70 and the C^α atoms of SODD were kept fixed in space and restraints for the conserved contacts of the residues mentioned above were applied. Molecular dynamics of the system was simulated for 1 ns with AMBER5 using TP3 water. For the dynamics simulation the SODD restraints on C^α atoms were released, allowing the domain itself to move, while additional HN-O restraints in α-helical regions and a few helix–helix restraints were introduced in this calculation to stabilize secondary and tertiary structure.

3. Results and discussion

3.1. Chemical shift assignment and secondary structure

An almost complete resonance assignment of proton, carbon and nitrogen resonances was achieved by a combined evaluation of amino acid-selective HSQC and standard 3D triple resonance experiments. Chemical shift-based approaches of secondary structure prediction by PLATON and TALOS identified three α-helices from S379–F400, D406–D424 and G430–K454 which were confirmed by the characteristic medium-range NOE pattern. A plot of the chemical

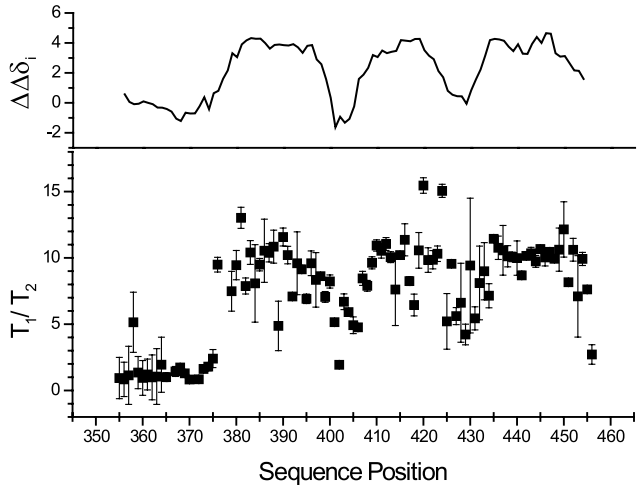

Fig. 2. Chemical shift distribution and local flexibility of the construct. The upper panel shows the chemical shift distribution for C_α and C_β as determined by Eq. 1. Positive values are indicators for α-helical secondary structure. The lower panel shows the ratio of T_1/T_2 ^{15}N relaxation times as a measure for local flexibility. Lower values indicate higher flexibility.

shift deviations highlights these predictions (Fig. 2), and shows a difference for the positions of the first helix and the loop between helices 1 and 2 in our structure as compared to the original alignments [2].

3.2. Solution structure and backbone dynamics of the SODD BAG domain

The structure of the SODD BAG domain was determined on the basis of 923 inter-residue NOE-derived distance restraints, H-bond restraints and dihedral angle restraints generated by TALOS (for details see Table 1). As expected from the sequence alignments and the 3D structures of hBag1 [8] and mBag1 [7] the BAG domain of SODD is exclusively α-helical and forms a three-helix bundle (Fig. 3) as also found by Briknarova et al. [9]. The ensemble of 20 structures, lowest in energy of 400 calculated structures, shows an average RMSD to the mean structure of 0.5 Å for the backbone atoms and 1.1 Å for the side chain heavy atoms (Table 2). The hydrophobic core of the domain is formed by residues I383, V386, V390, L393, V397, F400, Y409, L412, L416, L423, V426, A441, I445, I448, L449 and L452. Residues F400 and Y409, which are conserved in all short BAG domains, seem to play a key role in stabilizing the loop between the helices α1 and α2. The helix boundaries were found at residues S379–F400, D406–D424 and Q431–K455 respectively. In a structural alignment based on conserved residues (Fig. 4) these helices align well with those of Bag1. The N-terminus G353–T376 of our construct is unstructured as indicated by the lower T_1/T_2 ratios measured from the relaxation rates (Fig. 2). Furthermore, these residues do not show any long-range NOEs. This demonstrates that the N-terminus

Table 1
Input data for structure calculation

Restraints	
NOEs	
Assigned NOEs	1314
Used for calculations	731
Intra-residue	583
Long-range	219
Medium-range	258
Sequential	254
Other	
H-bonds (from CSI)	52
Dihedrals (from TALOS)	140

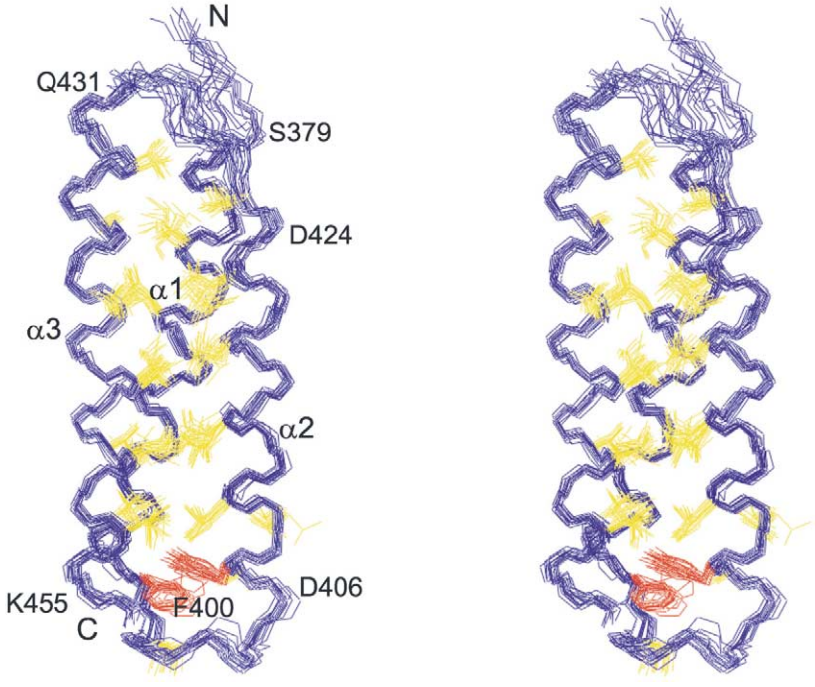

Fig. 3. Ensemble of the 20 lowest energy structures. The stereo picture shows the structures of the 20 structures with the lowest energy of 400 structures calculated by simulated annealing aligned to the coordinates of the backbone atoms. Hydrophobic core residues are depicted in yellow, the side chains of F400 and Y409 are colored in red. Figure generated with MOLMOL [26].

Table 2
Quality of the ensemble

RMSD (for residues 379–452): (from MOLMOL)	
Backbone atoms	0.5 ± 0.09 Å
Side chain heavy atoms	1.1 ± 0.09 Å
Deviation from idealized geometry: (from CNS)	
Bonds	0.0010 ± 0.00005
Angles	0.2858 ± 0.0029
Impropers	0.1651 ± 0.0083
Violations:	
Distances >0.2 Å	0
Dihedrals >5°	0
Ramachandran plot: (from Procheck NMR)	
Most favored regions	93.0%
Additionally allowed regions	7.0%
Generously allowed regions	0.0%
Forbidden regions	0.1%

of our construct does not belong to the BAG domain of SODD and its presence does not induce a shift of helix 1 to a position suggested by the original sequence alignment. Hence, the SODD BAG domain is indeed the structural prototype of a short BAG domain subfamily [29].

3.3. *The structure of the SODD BAG domain defines a new subfamily of BAG domains and shows a conserved HSP70 binding interface*

A structure-induced sequence alignment (Fig. 1) shows that all BAG domains exhibit a high conservation of the binding interface to HSP70 in the C-terminal part of the domain. In this alignment all BAG domains containing the motif F_i, Y_{i+9} as F400, Y409 in SODD-BAG were considered to belong to the shorter subfamily of BAG domains with a characteristic 19 amino acid deletion. Mapping of the conserved residues on the surface of the SODD BAG domain shows that all residues interacting specifically in the hBag1/HSP70 complex are conserved in SODD. This is shown in Fig. 5a–c in which conserved residues that are found to be essential for the interaction with HSP70 in the crystal or by mutagenesis experiments [8,9] are colored in blue while other residues conserved throughout the whole family are colored in cyan. SODD subfamily-specific residues are highlighted in green. The conservation of the non-subfamily-specific residues extends over all other BAG domains (Fig. 1). In the new SODD subfamily two glutamic acids E413 and E427 are also remarkably conserved, and W410 and E419 appear at the edges of the common binding interface to HSP70 (Fig. 5c). As a prerequisite for a conserved binding mode it would be expected that the electrostatic potential surfaces should be largely conserved. Indeed, many features of the charge distribution are similar (Fig. 5d,e). However, a remarkable difference is the larger negatively charged area due to E413 in the lower half of the interface as defined in Fig. 5a. The differences in the electrostatic properties of the binding site are conserved in the SODD subfamily, raising the question of whether the binding mode of this subfamily may indeed be the same as that found for hBag1.

3.4. *The homology model of the SODD-BAG/HSP70 complex reveals an extended interaction network in the HSP70 complexes of SODD subfamily BAG domains*

We built a homology model of the SODD-BAG/HSP70 complex [8] to address the question whether the differences in charge distribution between SODD and hBag1 BAG domains can be compensated in the complex or not. Since all residues in the interaction site that are found to mediate the contact between Bag1 and HSP70 are conserved throughout all BAG domains, we assume that the interaction with HSP70 remains the same for all of them. In our homology model which does not differ considerably from the hBag1/HSP70 complex, the two subfamily-specific negatively charged amino acids E413 and E427 in SODD are found to be able to form H-bonds/salt bridges to R258 and R269 in HSP70, respectively. All other non-conserved residues are involved in hydrophobic interactions. The network of H-bonds found in the complex structure of hBag1 is extended by these additional interactions (Fig. 6b). While E413 is within the protein interface, E427 is close to its edge and its interactions are thus interrupted during the dynamics simulation by the insertion of water molecules. On the other hand, the C^{α}–C^{α} distance between residues E427 and R269 remains within 13 Å which allows the formation of an H-bond or salt bridge between residues E427/R269. Our model shows thus that the additional charges in the binding interface of the SODD subfamily can be compensated or delocalized in the complex without chang-

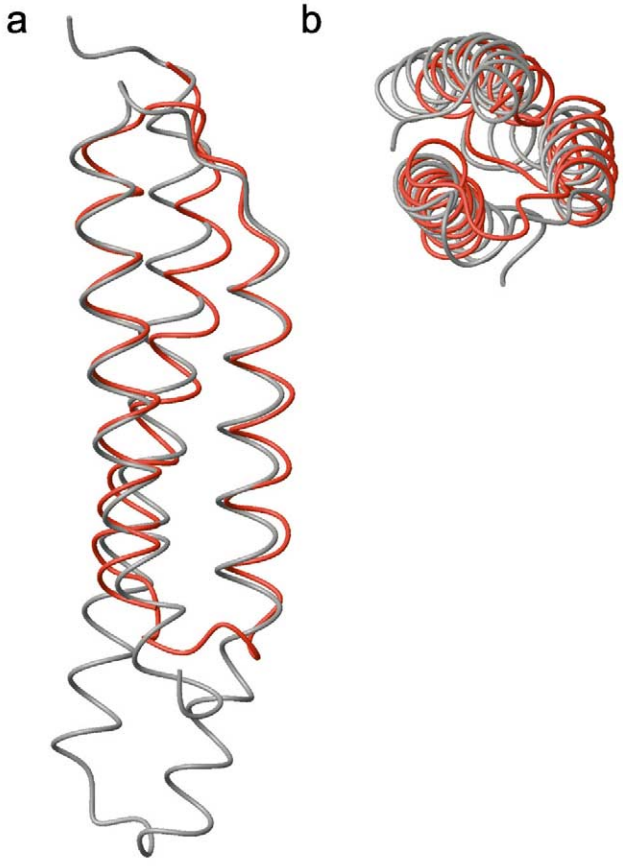

Fig. 4. Structural alignment. Structures of SODD and hBag1 (taken from 1HX1) BAG domains were aligned using the backbone atoms of residues 414, 420, 424, 435, 438, 446 and 453 in SODD and the corresponding residues in hBag1 which were shown to mediate the interaction with HSP70. The figure shows the binding interface (a) and the view from the N-terminus (b) rotated by 90° relative to a. Figure generated with MOLMOL.

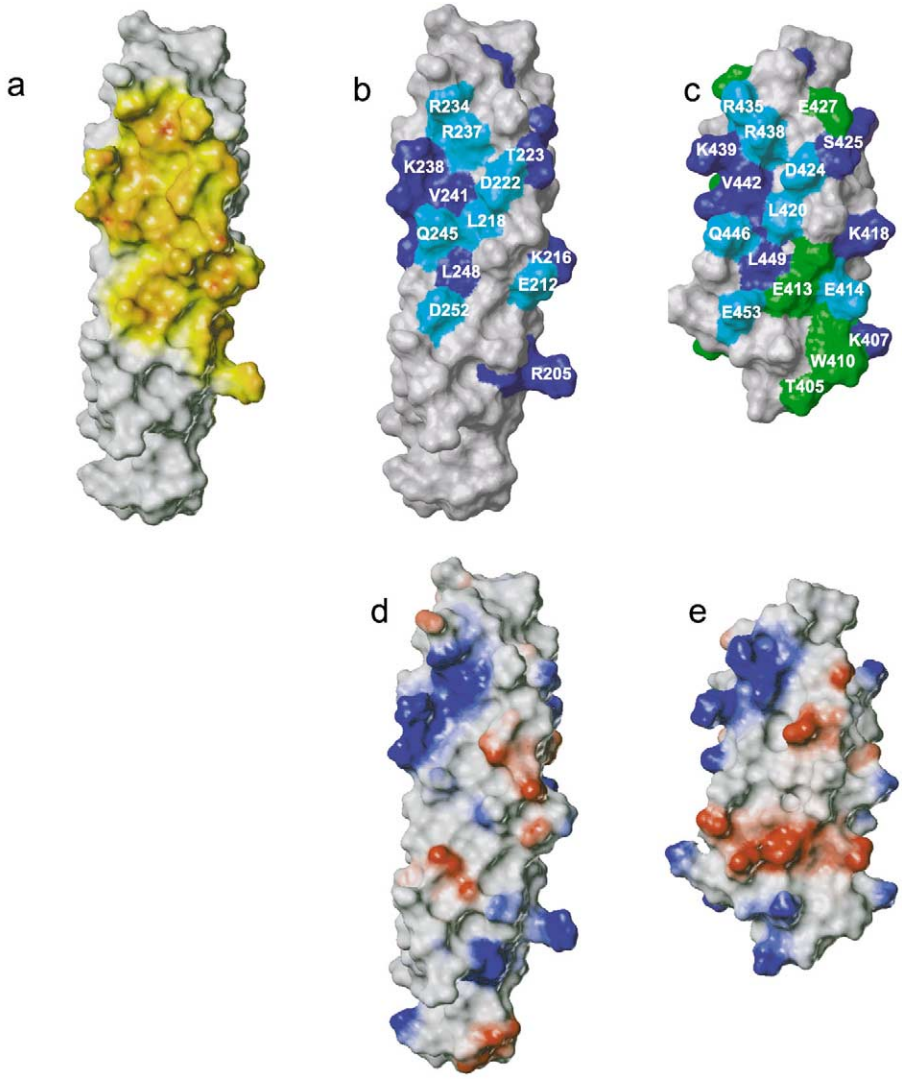

Fig. 5. Comparison of surface properties of the BAG domains of hBag1 and SODD. Surfaces of the BAG domains of hBag1 (a,b,d, taken from 1HX1) and SODD (c,e). In (a) the contact area of hBag1 to HSP70 in the crystal structure is depicted in orange. The conservation profile is mapped on the surface of the BAG domains in (b) and (c). Residues are colored as indicated in the text. In (d) and (e) the surfaces are colored according to electrostatic potential. The orientation is the same as in Fig. 3. Parts (b) and (c) were generated with MOLMOL.

ing its overall geometry. It is therefore likely that the geometry of the complex is conserved for all BAG domains. These charge differences might therefore modulate binding affinities to HSP70 of the two subfamilies as observed experimentally for mutants of interferon-α2 in its complex with ifnar2 [30]. In case the interface is used for other interactions they may ensure the binding of a different spectrum of interaction partners.

In summary, we have determined the solution structure and backbone dynamics of an N-terminally extended construct of the SODD BAG domain by NMR spectroscopy. The BAG domain of SODD is shorter by 19 amino acids between helices α1 and α2 as compared to that of hBag1. The presence of the N-terminal extension suggested by the original alignments to be part of the domain does not induce a shift of the first helix. It is therefore most likely the structural prototype of a SODD-like subfamily of BAG domains. In the SODD BAG domain there are two additional negative charges in the otherwise well conserved binding interface of BAG domains to their common interaction partner HSP70. A homology model of our domain in complex with HSP70 shows that these residues are likely to form additional contacts to the arginines R258 and R269 in HSP70. Interestingly, we found these glutamic acids conserved throughout the SODD subfamily. The presence of these residues may ensure different binding affinities for SODD and hBag1 BAG domains to HSP70 and, in case the interface is used for other interactions, ensure the binding of a different spectrum of interaction partners.

The structural coordinates have been deposited in the PDB with code 1M7K.

Acknowledgements: Special thanks to Martina Leidert, who prepared the samples, and Peter Schmieder for help with the pulse sequences. Thanks to Linda J. Ball for carefully reading the manuscript and Arvid Söderhäll for helpful discussions on model building. C.B. receives a grant from the DFG PhD Graduate Study Programme #788 'Hydrogen Bonding and Hydrogen Transfer'.

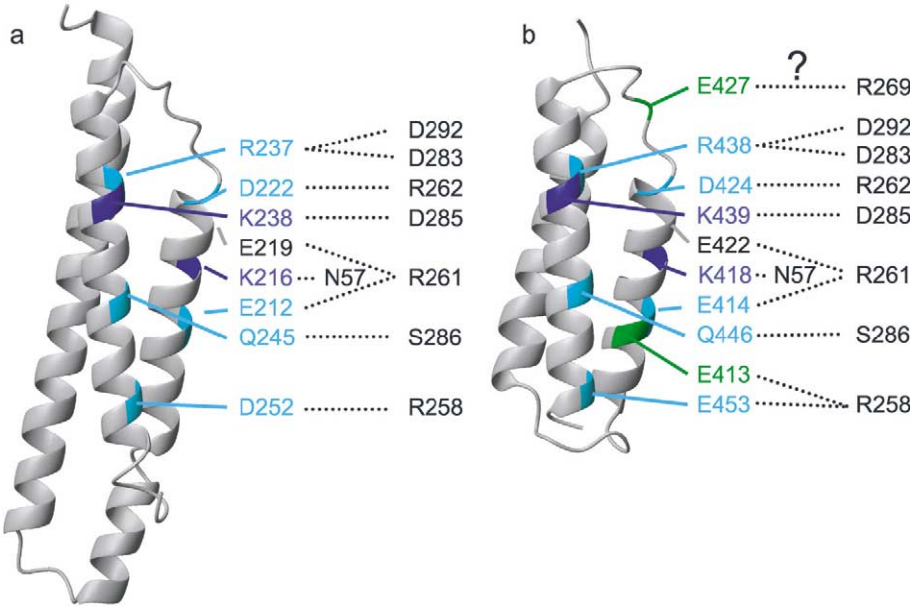

Fig. 6. Schematic plot of the H-bonded interactions in the hBag1- and SODD-BAG/HSP70 complexes. Residues that are found to mediate contacts in the respective complexes are colored according to Fig. 5. The residues of HSP70 can be found on the left side of the figures. H-bonding interactions in the complexes of hBag1 (a) and SODD (b) are indicated by dotted lines. Ribbon representations were generated with MOLMOL.

References

[1] Bateman, A., Birney, E., Cerruti, L., Durbin, R., Etwiller, L., Eddy, S.R., Griffiths-Jones, S., Howe, K.L., Marshall, M. and Sonnhammer, E.L. (2002) Nucleic Acids Res. 30, 276–280.
[2] Takayama, S., Xie, Z. and Reed, J.C. (1999) J. Biol. Chem. 274, 781–786.
[3] Antoku, K., Maser, R.S., Scully, W.J.Jr., Delach, S.M. and Johnson, D.E. (2001) Biochem. Biophys. Res. Commun. 286, 1003–1010.
[4] Jiang, Y., Woronicz, J.D., Liu, W. and Goeddel, D.V. (1999) Science 283, 543–546.
[5] Ozawa, F., Friess, H., Zimmermann, A., Kleeff, J. and Buchler, M.W. (2000) Biochem. Biophys. Res. Commun. 271, 409–413.
[6] Miki, K. and Eddy, E.M. (2002) Mol. Cell. Biol. 22, 2536–2543.
[7] Briknarova, K., Takayama, S., Brive, L., Havert, M.L., Knee, D.A., Velasco, J., Homma, S., Cabezas, E., Stuart, J., Hoyt, D.W., Satterthwait, A.C., Llinas, M., Reed, J.C. and Ely, K.R. (2001) Nat. Struct. Biol. 8, 349–352.
[8] Sondermann, H., Scheufler, C., Schneider, C., Hohfeld, J., Hartl, F.U. and Moarefi, I. (2001) Science 291, 1553–1557.
[9] Briknarova, K., Takayama, S., Homma, S., Baker, K., Cabezas, E., Hoyt, D.W., Li, Z., Satterthwait, A.C. and Ely, K.R. (2002) J. Biol. Chem. 277, 1528–1532.
[10] Schubert, M., Smalla, M., Schmieder, P. and Oschkinat, H. (1999) J. Magn. Reson. 141, 34–43.
[11] Schubert, M., Oschkinat, H. and Schmieder, P. (2001) J. Magn. Reson. 153, 186–192.
[12] Schubert, M., Oschkinat, H. and Schmieder, P. (2001) J. Magn. Reson. 148, 61–72.
[13] Grzesiek, S. and Bax, A. (1992) J. Am. Chem. Soc. 115, 11620–11621.
[14] Grzesiek, S. and Bax, A. (1992) J. Magn. Reson. 99, 201–207.
[15] Montelione, G.T., Lyons, B.A., Emerson, S.D. and Tashiro, M. (1992) J. Am. Chem. Soc. 114, 6291–6293.
[16] Kay, L.E., Ikura, M. and Bax, A. (2002) J. Am. Chem. Soc. 112, 888–889.
[17] Schmieder, P., Leidert, M., Kelly, M. and Oschkinat, H. (1998) J. Magn. Reson. 131, 199–202.
[18] Clore, G.M. and Gronenborn, A.M. (1992) Progr. Nucl. Magn. Reson. Spectrosc. 23, 43–92.
[19] Jenner, J., Meier, B.H., Bachmann, P. and Ernst, R.R. (1972) J. Chem. Phys. 71, 4546–4553.
[20] Goddard, T.D. and Kneller, D.G. (2002) SPARKY, University of California, San Francisco, CA.
[21] Farrow, N.A., Muhandiram, R., Singer, A.U., Pascal, S.M., Kay, C.M., Gish, G., Shoelson, S.E., Pawson, T., Forman-Kay, J.D. and Kay, L.E. (1994) Biochemistry 33, 5984–6003.
[22] Labudde, D., Leitner, D., Krüger, M. and Oschkinat, H. (2002) J. Biomol. NMR 25, 41–53.
[23] Cornilescu, G., Delaglio, F. and Bax, A. (1999) J. Biomol. NMR 13, 289–302.
[24] Metzler, W.J., Constantine, K.L., Friedrichs, M.S., Bell, A.J., Ernst, E.G., Lavoie, T.B. and Mueller, L. (1993) Biochemistry 32, 13818–13829.
[25] Brunger, A.T., Adams, P.D., Clore, G.M., DeLano, W.L., Gros, P., Grosse-Kunstleve, R.W., Jiang, J.S., Kuszewski, J., Nilges, M., Pannu, N.S., Read, R.J., Rice, L.M., Simonson, T. and Warren, G.L. (1998) Acta Crystallogr. D Biol. Crystallogr. 54, 905–921.
[26] Koradi, R., Billeter, M. and Wüthrich, K. (1996) J. Mol. Graphics 14, 51–55.
[27] Laskowski, R.A., Rullmannn, J.A., MacArthur, M.W., Kaptein, R. and Thornton, J.M. (1996) J. Biomol. NMR 8, 477–486.
[28] Pearlman, D.A., Case, D.A., Caldwell, J.W., Ross, W.S., Cheatham, T.E., DeBolt, S., Ferguson, D., Seibel, G. and Kollman, P. (1995) Comp. Phys. Commun. 91, 1.
[29] Tschopp, J., Martinon, F. and Hofmann, K. (1999) Curr. Biol. 9, R381–R384.
[30] Piehler, J., Roisman, L.C. and Schreiber, G. (2003) J. Biol. Chem. 275, 40425–40433.